Intrinsic Viscosity of Flexible Polymers in Unbounded and Bounded Newtonian Shear Flow

J. H. van Vliet and G. ten Brinke*

Department of Polymer Chemistry, University of Groningen, Nijenborgh 16, 9747 AG Groningen, The Netherlands

Received January 21, 1991; Revised Manuscript Received May 16, 1991

ABSTRACT: The zero-shear-rate intrinsic viscosity of a polymer in an athermal and Θ solvent in free space and confined in a slit is investigated by Monte Carlo simulations of self-avoiding random walks on a simple cubic lattice. The intrinsic viscosity in a Newtonian shear flow is calculated by Zimm's algorithm. The results for an unbounded system are in excellent agreement with several scaling predictions. The intrinsic viscosity is below its unbounded value when the coil is squeezed. The effect of hydrodynamic interactions between walls and chain segments on the intrinsic viscosity is negligible. The differences between Θ and athermal solvent conditions gradually diminish with a decrease in the width of the slit as witnessed by the intrinsic viscosity and the scaling exponent for the radius of gyration. This is due to the fact that the solvent quality improves for a decreasing slit width; i.e., a Θ solvent in three dimensions becomes a good solvent in two dimensions. The increase in excluded volume implies that there is a distinct difference between Θ chains (i.e., chains that behave as random walks in free space) and real random walks. In the latter case the value of the component of the radius of gyration parallel to the walls is independent of the slit width. For real Θ chains it increases.

Introduction

The behavior of polymer solutions in shear flow is of considerable practical and theoretical interest. Although shear flow itself is one of the simplest flow types known, the presence of a polymer component complicates the analysis considerably. In polymer science the practical interest in the zero-shear-rate intrinsic viscosity is largely motivated by the possibility to obtain an average of the molecular weight of the polymer solute even if its molecular weight is too high to obtain data by light scattering or osmotic measurements. Furthermore, the intrinsic viscosity provides information on the coil volume[1] or the architecture of the chain, e.g., linear, circular, star, or comb shaped.[2] Another research field is concerned with the influence of the polymer on the viscosity of the solution as in hydrodynamic chromatography,[3,4] enhanced oil recovery,[5] drag reduction,[6,7] and lubrication.

Especially in the latter class of problems, the effects of confinement are noteworthy, i.e., the tendency of the polymer to avoid small pores,[8-10] the relative increase of the polymer segment density in the center of a single pore,[11,12] and the orientation and squeezing of the polymer coils in a pore.[13] These phenomena lead to viscosities different from that of a system where the confinement is insignificant, i.e., where the distance between confining boundaries is much larger than the radius of gyration of a polymer coil.[5]

If the shear stress is not a constant, as in Poiseuille flow, the polymer chains prefer the regions with the lowest shear stress.[14,15] The discussion in this paper is limited to a planar unbounded or bounded flow at constant shear stress (Couette flow) in the Newtonian regime.

For a steady shear flow of a dilute polymer solution not too far from equilibrium, i.e., at low shear rates, the spatial distribution function of the polymer chain at rest is valid as shown by Kramers.[16] An assumption made first by Kramers and also used by others for this regime where Brownian motion is dominant is rigid body rotation of the polymer coil in the shear flow, i.e., the neglect of coupling between small-scale and center-of-mass motions.[16,17] The constant angular velocity for the segments of the polymer can be assumed a priori[17] or expressed as a configurational average of angular velocities.[18] On the basis of these assumptions the zero-shear rate intrinsic viscosity, $[\eta]_0$ (0 indicates the unconfined system), can be calculated. By introduction of the Oseen tensor, hydrodynamic interactions (HI) can be modeled. In the Kirkwood–Riseman approximation this tensor is preaveraged, allowing an analytical treatment of the problem.[18,19] To avoid this preaveraging, Zimm used a Monte Carlo procedure treating each conformation as a rigid body.[21] Wilemski et al.[22] and Fixman[23] showed that the Zimm procedure gives an upper bound of $[\eta]_0$. The Zimm procedure gives results for $[\eta]_0$ in good agreement with experimental and theoretical results in both off-lattice[24,25] and lattice simulations.[26] Therefore the calculation of $[\eta]_0$ is model independent as stated by Wilemski et al.[22] As a further test of Zimm's algorithm we calculated the scaling behavior of $[\eta]_0$ and compared it with experimental and theoretical predictions.

Modeling of a bounded Newtonian shear flow of dilute polymer solutions to calculate the zero-shear-rate intrinsic viscosity is far from trivial. The boundaries are two walls perpendicular to the Z direction and parallel to the direction of shear, X. The relation between the constant shear stress, σ, shear rate, $\dot{\gamma}$, and viscosity, η, is

$$\sigma = \eta\dot{\gamma} \quad \text{with } \dot{\gamma} = dv_x/dz \quad v_y = v_z = 0 \tag{1}$$

where v_α is the α component of the velocity field and $\alpha = x, y, z$. In an unbounded flow

$$\dot{\gamma}_0 = [v_x(L) - v_x(0)]/L \tag{2}$$

where L is the diameter of the slit. Due to the presence of boundary walls $\dot{\gamma}$ is not a constant as in free flow. The resulting velocity profile is pictured in Figure 1. Here we consider $\dot{\gamma}$ to be independent from Z. Such an approximation is not too bad as we are interested in the zero-shear-rate intrinsic viscosity, $[\eta]_L$, i.e., the limit $\dot{\gamma} \to 0$. For computational convenience HI and friction with the repulsive walls are usually assumed to be absent. In experiment these assumptions will break down when the distance between the walls is too small to neglect HI with the wall or to ignore slip of the solvent or the molecular nature of the polymer chain, wall, and solvent.[27-30] To ignore HI between chain segments and walls is not too

0024-9297/91/2224-5351$02.50/0

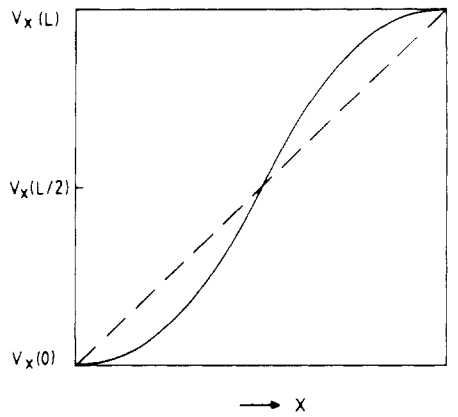

Figure 1. (- - -) Velocity profile in unbounded shear flow; (—) velocity profile in bounded shear flow.

drastic an approximation as will be argued further on in some detail.

On the basis of Casassa's work on the equilibrium segment distribution of a random-flight chain near a barrier, Chauveteau et al. proposed a two-layer model with the depleted layer nearby the wall having the lower viscosity.[5,11] The intrinsic viscosity in both layers is assumed equal. The thickness of the layer scales as the radius of gyration.[31] As noted by these authors and others,[32] the choice of the depleted layer thickness is somewhat arbitrary. Besides these semiempirical studies on pore flow, theoretical studies of polymer solutions in simple bounded shear flow, using an elastic or rigid dumbbell[33] as a model for the polymer chain,[34-41] have been published. These models describe the effect of the polymer on velocity and viscosity profiles and they can go beyond the Newtonian shear rate regime, i.e., further from equilibrium than our own model or the two-layer model of Chauveteau et al. Nevertheless complementary work is necessary as these dumbbell models and the two-layer model lack some essential features. So far HI between dumbbell beads has not been taken into account. As the dumbbell comprises only two beads, it is not a suitable model to describe the effect of polymer flexibility or solvent quality on viscosity. The effect of orientation and squeezing of polymer coils due to the confinement on the zero-shear-rate intrinsic viscosity has not been taken into account in the two-layer model.

Method

For bounded shear flow, Monte Carlo simulations of a self-avoiding random walk (SAW) on a simple cubic lattice with periodic boundary conditions in the X and Y directions were performed. The two parallel walls were perpendicular to the Z axis. In the case of an unbounded shear flow, also periodic boundary conditions in the Z direction were applied. The length of the lattice in the directions with periodic boundary conditions varied with the number of steps of the SAW considered. In all cases, this length exceeded the root mean-square end-to-end distance of the SAW. The number of steps of the SAW's considered were N = 19, 39, 59, 79, and 150 and for the unbounded system also N = 99 and 119. For each chain length considered, the lattice length in the X and Y directions was fixed. For the shortest distance between the walls considered, the densities, expressed as the fraction of lattice sites occupied, varied between 0.51% for N = 19 and 1.73% for N = 150. For greater distances between the walls or with periodic boundary conditions in the Z direction, the densities were correspondingly lower. For each chain length and distance between the walls, a representative sample was obtained by the reptation algorithm. To speed up equilibration, chain growth and reptation took place simultaneously. In the case of Θ chains the Metropolis sampling scheme was also used. Details of the method can be found in a review on Monte Carlo simulations of lattice chains and references therein.[42] For N = 150 simple randon walks (RW) were generated as for athermal SAW's with the possibility of multiple occupancy of a lattice site. The Θ condition was modeled by choosing a square potential, ϵ/kT, between two segments of a SAW one lattice distance apart in such a way that the mean-square radius of gyration, $\langle S^2 \rangle$, scales with the number of steps, N, connecting the $N+1$ segments of the chain as

$$\langle S^2 \rangle \sim N^{2\nu} \qquad \nu \equiv {}^1/_2 \tag{3}$$

The angular brackets indicate an average over all conformations concerned. The square potential is

$$\begin{aligned} \epsilon/kT &= \infty \qquad R = 0 \\ \epsilon/kT &= A \qquad R = 1 \\ \epsilon/kT &= 0 \qquad R > 1 \end{aligned} \tag{4}$$

where R is the distance between segments in lattice spacings. Choosing for A the value previously found by McCrackin et al., A = −0.275, gives a satisfactory result for ν (Table I).[43]

Table I
Scaling Exponents: Unbounded Flow[a]

	athermal solvent	Θ solvent
$\langle S^2 \rangle$	1.22 ± 0.02	1.05 ± 0.03
$[\eta]_0^{HI}$	0.67 ± 0.02	0.52 ± 0.02
$[\eta]_0^{FD}$	1.17 ± 0.03	1.03 ± 0.03

[a] N = 19, 39, 59, 79, 99, 119, and 150.

The first 2×10^6 attempted moves after completion of chain growth were ignored. From the subsequent interval of 2×10^6 attempted moves 26 times, at equally spaced intervals, quantities of interest were calculated and averaged afterward. This procedure was repeated for five independent runs. After averaging again, the statistical errors were calculated as usual from the averages per run.

The zero-shear-rate intrinsic viscosity was calculated by Zimm's procedure.[21] The method is essentially the same as that of Wilkinson et al.[26] We also used the same expression for the elements of the Oseen tensor.[44,45]

The polymer coil is considered to be a rigid body. Rotation is hindered when two conditions are satisfied. The first condition is that one or more segments of the SAW are in a lattice layer one step length apart from either of the boundary walls. The second condition is that for at least one of these segments the coordinate in the direction of shear relative to the center of mass of the SAW is positive in one layer or negative in the other. Due to symmetry it is irrelevant which layer is associated with which sign of the segment coordinate, but the coupling should be fixed during one computer run. If rotation is hindered we assume for the angular velocity $\omega = 0$. Then the whole coil only has a translational velocity component equal to the velocity of the center of mass. The basic equations can be found elsewhere;[20,21] however, to clarify the above considerations we will give a brief overview of equations involved:

$$\mathbf{v}_i = \mathbf{v}_i^0 + \mathbf{v}_i^* \tag{5}$$

$$\mathbf{F}_i = \zeta(\mathbf{u}_i - \mathbf{v}_i) \qquad \zeta = 6\pi\eta_0 a \qquad \eta_0 = 1 \tag{6}$$

$$\mathbf{v}_i^* = \sum_{i \neq j}^{N+1} \mathbf{T}_{ij}\mathbf{F}_j \tag{7}$$

where $\mathbf{v}_i^0$ is the velocity of the solvent at the position of the ith segment if that segment would have been absent, $\mathbf{u}_i$ is the velocity of the ith segment, ζ is the friction coefficient, η_0 is the solvent viscosity, a is the Stokes radius of a segment in step length units ($a = 1/2$), $\mathbf{F}_i$ is the friction force exerted on the solvent, $\mathbf{v}_i^*$ is the contribution to $\mathbf{v}_i$ due to hydrodynamic perturbation from all other segments of the polymer chain and $\mathbf{T}$ is the Oseen tensor. Equations 5–7 give the equation to be solved numerically,[21] with HI

$$(1/\zeta)\mathbf{F}_i + \sum_{i \neq j}^{N+1} \mathbf{T}_{ij}\mathbf{F}_j = \mathbf{u}_i - \mathbf{v}_i^0 \tag{8}$$

or with free draining (FD)

$$(1/\zeta)\mathbf{F}_i = \mathbf{u}_i - \mathbf{v}_i^0 \tag{9}$$

If rotation is possible, $\omega = \dot{\gamma}/2$, the components of $\mathbf{v}_i^r = \mathbf{u}_i - \mathbf{v}_i^0$ are

$$v_{i,x}^r = (-\dot{\gamma}/2)z_i \qquad v_{i,y}^r = 0 \qquad v_{i,z}^r = (-\dot{\gamma}/2)x_i \tag{10}$$

if rotation is impossible, $\omega = 0$

$$v_{i,x}^r = -\dot{\gamma}z_i \qquad v_{i,y}^r = 0 \qquad v_{i,z}^r = 0 \tag{11}$$

where x_i and z_i are the coordinates relative to the coil's center of mass.

For the dimensionless quantity $E_L \sim [\eta]_L$ actually computed one gets

$$\text{for } \omega = \dot{\gamma}/2: \qquad E_L = -\sum_{i}^{N+1}(x_i F_{i,z} + z_i F_{i,x})/2(N+1) \tag{12}$$

$$\text{for } \omega = 0: \qquad E_L = -\sum_{i}^{N+1} z_i F_{i,x}/(N+1) \tag{13}$$

Therefore the statistical fluctuations in E_L with eq 12 are less than with eq 13.[21]

For an athermal SAW with $N = 150$ also HI between chain segments and the wall was taken into account in order to prove that the neglect of this HI is justified. The HI of a segment with each of the walls is modeled as the HI of a solid sphere with a wall. As $a = 1/2$ and the distance d_i between one of the walls and the ith segment in step length units satisfies $d_i \geq 1$, results on HI published for $a/d_i \ll 1$ are used. Corrections to the HI with both walls are superimposed and only terms linear in a/d_i are retained for the diagonal elements of the Oseen tensor.[46]

No HI between segments and the walls:

$$T_{ii}^{xx} = T_{ii}^{yy} = T_{ii}^{zz} = 1/\zeta \tag{14}$$

HI between segments and the walls:

$$T_{ii}^{xx} = T_{ii}^{yy} = (1/\zeta)\left(1 - \frac{9}{16}\frac{aL}{(L-d_i)d_i} + \ldots\right) \tag{15}$$

$$T_{ii}^{zz} = (1/\zeta)\left(1 - \frac{9}{8}\frac{aL}{(L-d_i)d_i} + \ldots\right) \tag{16}$$

Table II
Influence of Chain Model and L^a

L	chain	$\langle S^2\rangle$	$\langle S_\perp{}^2\rangle$	$\langle S_\parallel{}^2\rangle$	E^{FD}	E^{HI}
3	athermal	123	0.246	61.5	4.638	3.51
	Θ	79	0.247	39.5	4.66	3.33
	RW	20.9	0.245	10.3		
5	athermal	84	0.92	42	16.8	7.65
	Θ	47	0.887	23.1	19	7.2
	RW	18.5	0.76	8.9		
9	athermal	68	2.89	33	72	18.8
	Θ	36	2.6	17	55.0	14.0
	RW	19	2.26	8.4		
17	athermal	61	8.3	26	177	35
	Θ	35	6.9	14.3	166	23
	RW	23	4.6	9.0		
∞	athermal	71	24.3	24.3	200	40
	Θ	43	14.3	14.3	131	26
	RW	26	8.7	8.7		

[a] $N = 150$; $\langle S^2\rangle \equiv \langle S_\perp{}^2\rangle + 2\langle S_\parallel{}^2\rangle$.

Results and Discussion

Characteristic lengths of athermal SAW's in three dimensions, like $\langle S^2\rangle$, are known to scale according to eq 3, with $\nu = 0.6$.[47,48] The most accurate value available to date for a simple cubic lattice is 0.592.[49] For a SAW under Θ conditions, as described above, $\nu \equiv 1/2$. Therefore to compare results for different values of N, the distance between the walls is expressed in units Δ, defined by

$$\Delta \equiv L/N^\nu \tag{17}$$

athermal SAW: $\nu = 0.592$

Θ SAW: $\nu = 0.5$

With nondraining, i.e., infinite HI, the scaling behavior of $[\eta]_0$ is predicted to be[50]

$$[\eta]_0 \sim N^{3\nu-1} \tag{18}$$

With FD the scaling relation, using Debye's[17] results and eq 3, is

$$[\eta]_0 \sim N^{2\nu} \tag{19}$$

For the HI and for the FD calculations the agreement between our results (Table I) and the scaling predictions is very good. The scaling exponents were obtained by linear regression according to

$$\langle \mathrm{Ln}\,(Q)\rangle = \mathrm{Ln}\,(C) + \alpha\,\mathrm{Ln}\,(N) \tag{20}$$

where Q is the quantity of interest, and α is its scaling exponent.

For the athermal solvent/HI case the scaling exponent is in the range experimentally observed[51] but less than 0.8, the value actually predicted, eq 18. The discrepancy is likely to be due to partial draining, i.e., finite HI in good solvents.[52] As noted by Freed the difference between $[\eta]_0$ with FD and $[\eta]_0$ with HI is less for the Θ than for the athermal solvent, due to the larger average distance between segments for the latter case (Table II).[53]

For an ideal chain, a RW confined in a slit, de Gennes predicted that for each distance L between boundary walls considered[48]

$$\langle S_\parallel{}^2\rangle = 1/3\langle S_0{}^2\rangle \qquad b \ll S \ll L \tag{21}$$

where b is the length of a statistical segment and $\langle S_\parallel{}^2\rangle$ is the component of $\langle S^2\rangle$ parallel to boundary walls. Our results for $\langle S_\parallel{}^2\rangle$ of RW's confirm this prediction. However, for a Θ chain $\langle S_\parallel{}^2\rangle$ increases when L decreases as for an athermal SAW (Table II). The remarkable difference between Θ chains and RW's can be ascribed to an increase

Table III
Scaling Exponents $\langle S^2 \rangle$[a]

L	athermal solvent	Θ solvent
3	1.5	1.3
5	1.4	1.1
9	1.2	1.0
17	1.2	1.0
∞	1.22	1.05

[a] N = 19, 39, 59, 79, and 150.

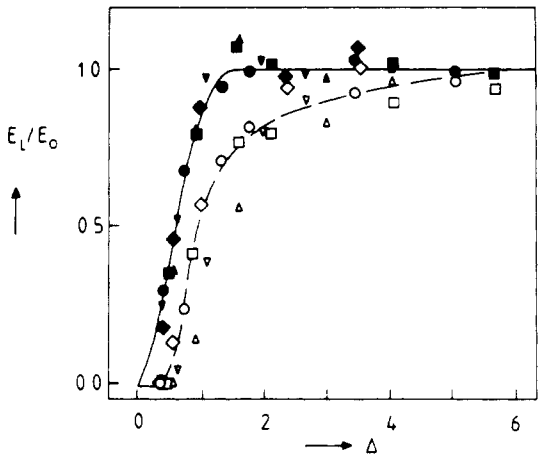

Figure 2. E_L/E_0 as a function of Δ for an athermal solvent and HI: (▲,△) N = 19; (▼,▽) N = 39; (■,□) N = 59; (●,○) N = 79; (♦,◇) N = 150. Open symbols and broken line: contribution from free rotation. Maximum error is 0.1.

of excluded volume with a decreasing value of L. The increase is due to the higher segment density for the SAW if it would have its RW dimensions at such a lower value of L.[54] Stated alternatively, the theta temperature, Θ, decreases going from a three-dimensional to a two-dimensional system. In a crude lattice mean field approximation, assuming ϵ to be constant, a simple argument based on the reduction in lattice coordination number from q = 6 to q = 4 leads to

$$\frac{\Theta(\text{square})}{\Theta(\text{cubic})} = \frac{1}{2} \tag{22}$$

The increase in excluded volume causes an increase in the scaling exponent for $\langle S^2 \rangle$ with a decrease in L for both athermal and Θ conditions (Table III). The increase in excluded volume also reduces the difference in intrinsic viscosity for athermal and Θ chains (Table II). A scaling analysis of the effect of confinement on $\langle S^2 \rangle$ of Θ chains was recently published.[55]

The influence of confinement on zero-shear-rate intrinsic viscosity is discussed in terms of $E_L/E_0 = [\eta]_L/[\eta]_0$. Figures 2–5 show E_L/E_0 as a function of Δ. Results for FD as well as results for HI are presented. Also the E_L/E_0 contribution of the chains freely rotating in the X,Z plane is given. For both Θ and athermal solvent conditions with Δ exceeding 1.5 a value of E_L/E_0 = 1 is reached (Figures 2–5). For Θ as well as athermal SAW's, with Δ exceeding 5, the contribution of freely rotating chains to E_L/E_0 is 1. Although there is a considerable scatter in the data due to statistical errors, Figures 2–5 clearly demonstrate a universal behavior as a function of Δ for all SAW's considered. For N = 19 the freely rotating chain contribution to E_L/E_0 is slightly below the universal curve probably because this contribution has not yet reached its large-chain limit.

This behavior is in agreement with our results on conformational properties of athermal SAW's presented in a

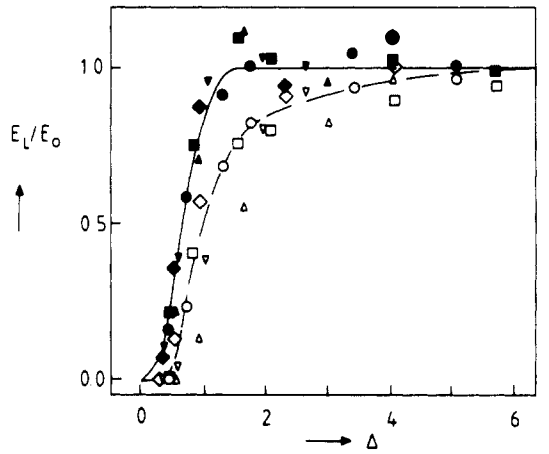

Figure 3. E_L/E_0 as a function of Δ for an athermal solvent and FD: (▲,△) N = 19; (▼,▽) N = 39; (■,□) N = 59; (●,○) N = 79; (♦,◇) N = 150. Open symbols and broken line: contribution from free rotation. Maximum error is 0.1.

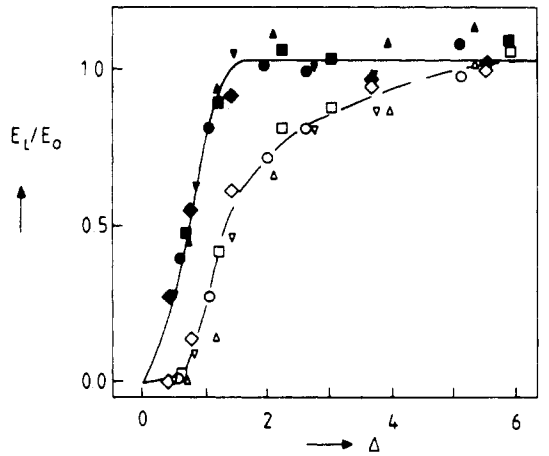

Figure 4. E_L/E_0 as a function of Δ for a Θ solvent and HI: (▲,△) N = 19; (▼,▽) N = 39; (■,□) N = 59; (●,○) N = 79; (♦,◇) N = 150. Open symbols and broken line: contribution from free rotation. Maximum error is 0.1.

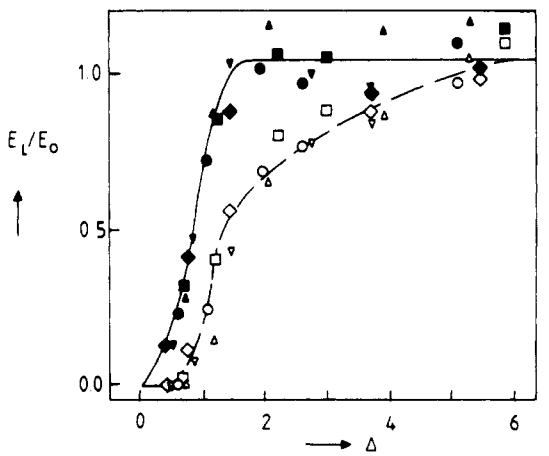

Figure 5. E_L/E_0 as a function of Δ for a Θ solvent and FD: (▲,△) N = 19; (▼,▽) N = 39; (■,□) N = 59; (●,○) N = 79; (♦,◇) N = 150. Open symbols and broken line: contribution from free rotation. Maximum error is 0.1.

previous paper[13] where it was demonstrated that $\langle S^2 \rangle$, the eigenvalues of the square radius of gyration matrix, and the orientation of the principal axes of the coil show universal behavior as a function of Δ. Remarkably, this corresponding-state behavior is valid over the entire Δ range, including the limit Δ → 0, for both conformational

properties and intrinsic viscosity. For Θ chains the conformational properties are essentially the same as those for athermal SAW's;[13] i.e., decreasing the width of the slit, the coil starts, due to its anisotropic shape, to orient long before its shape changes. Only after the longest principal axis is aligned considerably parallel to the walls the coil is squeezed. As mentioned before, a Θ solvent for a polymer ceases to be a Θ solvent in a strongly confined situation. The solvent quality improves with decreasing slit width and "Θ chains" start to behave as chains in good solvent, in clear contrast to random walks. For both athermal and Θ SAW's the coils are oriented for $\Delta \leq 2.5$ and squeezed for $\Delta \leq 1.5$. The squeezing of the coils clearly coincides with a decrease of $[\eta]_L$. The contribution of rotating polymer conformations to the viscosity already decreases for $\Delta \leq 5$. Therefore the conformations close to the walls still contribute considerably to $[\eta]_L$ even for $\Delta \geq 1.5$.

For an athermal chain with $N = 150$ no significant difference between results on E_L obtained with and without HI with the walls is observed in the range $L = 5$–67 ($\Delta = 0.26$–3.45). Basically, this seems to be due to the tendency of the polymer segments to concentrate in the center of the slit, away from the walls.

The effects of solvent quality, hydrodynamic interactions, and chain flexibility have not been considered so far in dumbbell models. As far as length scales are concerned the difference with the dumbbell is considerable. In Brunn's model the so-called "large-channel limit" for the viscosity is reached when the ratio of the diameter of the slit to the undisturbed end-to-end point distance $L/R_0 \geq 20$, and the dumbbell behaves almost completely unbounded for $L/R_0 \geq 100$.[36,38] In our model the influence of the walls vanishes at distances $\Delta \geq 5$, which corresponds to $L/R_0 \geq 4.7$ for an athermal chain[49] and $L/R_0 \geq 3.8$ for a Θ chain;[43] $[\eta]_L$ reaches its unbounded value $[\eta]_0$ at $\Delta \geq 1.5$. The difference is likely to be a consequence of the inflexibility of a dumbbell as compared to a lattice chain.

As a sliding chain segment experiences a larger friction force than a rotating one, its contribution to $[\eta]_L$ is larger than for a rotating segment. This explains the capability of even a small fraction of sliding conformations to contribute considerably to $[\eta]_L$. It probably also accounts for the tendency of E_L/E_0 to be slightly higher than 1 for Δ not too large (Figures 2–5), although the data scatter does not allow any definite conclusion.

Concluding Remarks

Although simplifying approximations have been made about the velocity profile, the calculation of the intrinsic viscosity, and the interaction with the walls, our model allows some reasonable conclusions to be drawn for the Newtonian shear regime considered.

It is clear that the effect of HI with the walls can be neglected as far as intrinsic viscosity is concerned, due to the low segment concentration near the walls. However, it should be realized that if HI is strong or if an attractive interaction between walls and polymer segments exists, results are likely to differ considerably from those obtained here.

For distances Δ between walls satisfying $\Delta \leq 1.5$, where the coil is squeezed, $[\eta]_L$ drops below its free-flow value $[\eta]_0$. The distance is far less than the corresponding length scale derived for dumbbells, due to the inherent lack of flexibility of the latter. For a pore with $\Delta = 1.5$ in equilibrium with a bulk solution, the fraction of random-flight conformations in the pore is only slightly less than in the bulk,[8-10] indicating the relevance of studying polymer solutions confined in small pores.

The drop of $[\eta]_L$ as $\Delta < 1.5$ might be useful in the determination of the radius of gyration of a polymer coil in solution by determination of $[\eta]_L$ as a function of distance between plates in a Couette-type viscometer. This might be especially useful with high polymers with a radius of gyration too large to be determined by the classical light scattering method.[56]

The effect of solvent quality and hydrodynamic interaction on coil conformations and intrinsic viscosity diminishes for $\Delta \to 0$. This is due to the increase of the solvent quality with a decrease of L. Furthermore, due to squeezing, coils with a distance $\Delta \leq 0.75$ between the center of mass and a wall have an intrinsic viscosity less than $[\eta]_0$, a fact that seems relevant for two-layer models but that has not been taken into consideration so far.[5,31,32]

Acknowledgment. We thank Dr. J. F. Douglas for some useful comments.

References and Notes

(1) Weill, G.; Des Cloiseaux, J. *J. Phys. (Les Ulis, Fr.)* **1979**, *40*, 99.
(2) Douglas, J. F.; Roovers, J.; Freed, K. F. *Macromolecules* **1990**, *23*, 4168.
(3) Small, H. *J. Colloid Interface Sci.* **1974**, *48*, 147.
(4) Di Marzio, E. A.; Guttman, C. M. *Macromolecules* **1970**, *3*, 131.
(5) Chauveteau, G.; Tirrell, M.; Omari, A. *J. Colloid Interface Sci.* **1984**, *100*, 41.
(6) Zakin, J. L.; Hunston, D. L. *J. Macromol. Sci., Phys.* **1980**, *B18*, 795.
(7) Block, H. *Molecular Behavior and the Development of Polymeric Materials*; Ledwith, A., North, A. M., Eds.; Chapman & Hall: London, 1975.
(8) Casassa, E. F. *Polym. Lett.* **1967**, *5*, 773.
(9) Casassa, E. F.; Tagami, Y. *Macromolecules* **1969**, *2*, 14.
(10) Davidson, M. G.; Suter, U. W.; Deen, W. M. *Macromolecules* **1987**, *20*, 1141.
(11) Casassa, E. F. *Macromolecules* **1984**, *17*, 601.
(12) Clark, A. T.; Lal, M. *J. Chem. Soc., Faraday. Trans.* **1981**, *77*, 981.
(13) Van Vliet, J. H.; ten Brinke, G. *J. Chem. Phys.* **1990**, *93*, 1436.
(14) Tirrell, M.; Malone, M. F. *J. Polym. Sci., Polym. Phys. Ed.* **1977**, *15*, 1569.
(15) Metzner, A. B.; Cohen, Y.; Rangel-Nafaile, C. *J. Non-Newtonian Fluid Mech.* **1979**, *5*, 449.
(16) Kramers, H. A. *J. Chem. Phys.* **1946**, *14*, 415.
(17) Debye, P. *J. Chem. Phys.* **1946**, *14*, 636.
(18) Muthukumar, M. *J. Phys. A: Math. Gen.* **1981**, *14*, 2129.
(19) Kirkwood, J. G.; Riseman, J. *J. Chem. Phys.* **1948**, *16*, 565.
(20) Yamakawa, H. *Modern Theory of Polymer Solutions*; Harper & Row: New York, 1971.
(21) Zimm, B. H. *Macromolecules* **1980**, *13*, 592.
(22) Wilemski, G.; Tanaka, G. *Macromolecules* **1981**, *14*, 1531.
(23) Fixman, M. *J. Chem. Phys.* **1983**, *78*, 1588.
(24) Garcia de la Torre, J.; López Martinez, M. C.; Tirado, M. M.; Freire, J. J. *Macromolecules* **1984**, *17*, 2715.
(25) Rey, A.; Freire, J. J.; Garcia de la Torre, J. *Macromolecules* **1987**, *20*, 342.
(26) Wilkinson, M. K.; Gaunt, D. S.; Lipson, J. E. G.; Whittington, S. G. *Macromolecules* **1988**, *21*, 1818.
(27) Bitsanis, I.; Magda, J. J.; Tirrell, M.; Davis, H. T. *J. Chem. Phys.* **1987**, *87*, 1733.
(28) Israelachvili, J. N.; Kott, S. J. *J. Colloid Interface Sci.* **1989**, *129*, 461.
(29) Gee, M. L.; McGuiggan, M.; Israelachvili, J. N.; Homola, A. M. *J. Chem. Phys.* **1990**, *93*, 1895.
(30) Hess, S.; Loose, W. *Physica A* **1989**, *162*, 138.
(31) Omari, M.; Moan, M.; Chauveteau, G. *Rheol. Acta* **1989**, *28*, 520.
(32) Sorbie, K. S. *J. Colloid Interface Sci.* **1990**, *139*, 299.
(33) Bird, B. R.; Curtiss, C. F.; Armstrong, R. C.; Hassager, O. *Dynamics of Polymer Solutions*, 2nd ed.; John Wiley & Sons: New York, 1987; Vol. 2.
(34) Brunn, P. O. *Rheol. Acta* **1976**, *15*, 23.
(35) Brunn, P. O.; Grisafi, S. *Chem. Eng. Commun.* **1985**, *36*, 367.
(36) Brunn, P. O. *J. Rheol.* **1985**, *29*, 859.
(37) Brunn, P. O.; Grisafi, S. *J. Non-Newtonian Fluid Mech.* **1987**, *24*, 343.
(38) Grisafi, S.; Brunn, P. O. *J. Rheol.* **1989**, *33*, 47.
(39) Aubert, J. H.; Tirrell, M. *J. Chem. Phys.* **1982**, *77*, 553.

(40) Park, O.; Fuller, G. G. *J. Non-Newtonian Fluid Mech.* **1984**, *15*, 309.
(41) Goh, C. J.; Atkinson, J. D.; Phan-Thien, N. *J. Chem. Phys.* **1985**, *82*, 988.
(42) Kremer, K.; Binder, K. *Comput. Phys. Rep.* **1988**, *7*, 260.
(43) McCrackin, F. L.; Mazur, J.; Guttman, C. M. *Macromolecules* **1973**, *6*, 859.
(44) Rotne, J.; Prager, S. *J. Chem. Phys.* **1969**, *50*, 4831.
(45) Felderhof, B. U. *Physica A* **1977**, *89*, 373.
(46) Faxen, H. *Arkiv. Mat. Astron. Fys.* **1923**, *17*, No. 27. O'Neill, M. E. *Mathematika* **1964**, *11*, 67. Goldman, A. J.; Cox, R. G.; Brenner, H. *Chem. Eng. Sci.* **1961**, *16*, 242. Lorentz, H. A. *Abhandl. Theoret. Phys.* **1906**, *1*, 23. Brenner, H.; Cox, R. G. *Chem. Eng. Sci.* **1967**, *22*, 1753. Clark, A. T.; Lal, M.; Watson, G. M. *Faraday Discuss. Chem. Soc.* **1987**, *83*, 179.
(47) Flory, P. *Principles of Polymer Chemistry*; Cornell University Press: Ithaca, NY, 1972; Chapter XII.
(48) de Gennes, P. G. *Scaling Concepts in Polymer Physics*; Cornell University Press: Ithaca, NY, 1979.
(49) Rapaport, D. C. *J. Phys. A: Math. Gen.* **1985**, *18*, 113.
(50) Kuhn, W. *Kolloid Z.* **1933**, *62*, 269; **1934**, *68*, 2. Kuhn, W.; Kuhn, H. *Helv. Chim. Acta* **1943**, *26*, 194.
(51) Brandrup, J.; Immergut, E. H., Eds. *Polymer Handbook*, 3rd ed.; John Wiley & Sons: New York, NY, 1989; VII/5–VII/32.
(52) Berry, G. C. *J. Chem. Phys.* **1967**, *46*, 1338. Freed, K. F.; Wang, S. Q.; Roovers, J.; Douglas, J. F. *Macromolecules* **1988**, *21*, 2219.
(53) Freed, K. F. *Renormalization Group Theory of Macromolecules*; John Wiley & Sons: New York, NY, 1987.
(54) Candau, F.; Rempp, P.; Benoit, H. *Macromolecules* **1972**, *5*, 627.
(55) Roby, F.; Johner, A. *C. R. Acad. Sci. Paris, (Ser. II)* **1991**, *312*, 1083.
(56) Tanford, C. *Physical Chemistry of Macromolecules*; John Wiley & Sons: New York, NY, 1961.